Pergamon

Int. J. Heat Mass Transfer. Vol. 37, Suppl. 1, pp. 415–423, 1994

0017–9310/94 $6.00+0.00

0017–9310(93)E0084–T

An analysis of conjugate heat transfer from a heated wall in a channel with zero-mean oscillatory flow for small oscillatory flow Reynolds numbers

Q. D. LIAO, K. T. YANG and V. W. NEE

Thermal Packaging Laboratory, Department of Aerospace and Mechanical Engineering, University of Notre Dame, Notre Dame, IN 46556, U.S.A.

Abstract—An exact solution for small oscillatory flow Reynolds numbers is presented for the fully-developed zero-mean oscillatory flow and heat transfer in a two-dimensional channel with a wall uniformly heated to simulate the forced-convection cooling of electronic components on printed circuit boards. The other channel wall is insulated and all thermal properties are taken to be constant. Also, results are given in terms of time-averaged Nusselt number as functions of oscillatory flow Reynolds number and Wormersely number, based on both channel height and tidal displacement as the characteristic lengths, and for two specific cases with air and water as the cooling fluid media.

INTRODUCTION

SINCE the development of more complex, large- and very large-scale integration technologies, there has been a steady increase in heat dissipation at the chip, module, and system levels. Such increase has made the role of heat transfer and thermal design more important than ever, and future development may well be limited by the inability to maintain effective cooling. The conventional cooling methods of electronic equipment, such as conduction, natural and steady state forced convection cooling, have been studied in great detail. Incropera [1] provided a comprehensive review of convection cooling options in electronic equipment cooling. To maintain the best possible thermal environment in electronic package, the engineer must establish the most efficient path for heat transfer from the electronic device to an external cooling agent. In recent years, a new cooling technique, utilizing a zero-mean oscillatory flow field for forced convection cooling of electronic equipment, has been reported in several studies. Zhang and Kurzweg [2], Kaviany [3], Kaviany and Reckker [4] have separately studied the problem of enhanced axial heat transfer in oscillatory pipe flow, and shown that the enhanced axial heat transfer can be several orders of magnitude higher than that possible with heat pipes. Kurzweg [5] also examined analytically the hydrodynamics of enhanced longitudinal heat transfer through a sinusoidally oscillating flow in an array of parallel-plate channels with conducting sidewalls and showed that the process discussed involved no net convection and hence achieved large heat transfer rates without a corresponding net convective mass transfer. Karniadakis *et al.* [6] used channel flow destabilization with cylindrical promoters to determine heat transfer enhancement in the case of chip cooling. Amon [7, 8] used a groved channel to approach an electronic packaging model composed of parallel printed circuit boards, and investigated the heat transfer enhancement induced by self-sustained oscillatory flow. It is found that on an equal pumping power basis, the heat transfer in communicating self-sustained oscillatory flow is up to 300% higher than the one in steady flat channel flow. Cooper *et al.* [9] experimentally investigated the convective heat transfer from a heated floor section of a rectangular duct into a low frequency, large tidal displacement oscillatory flow, and presented phase correlated profiles of the oscillatory velocity and temperature and a nondimensional correlation for both the oscillatory heat transfer coefficients and Nusselt numbers. Walsh *et al.* [10] introduced a fully oscillatory air flow device to forced convection cooling of the microcomputer cabinet, and, in some cases, component operating temperatures were improved as much as 40% using this oscillatory flow device. Liao *et al.* [11] had experimentally investigated the effectiveness of microcomputer 'hot spots' cooling using a new oscillatory flow device with or without additional channels, and also formulated the nondimensional temperature rise ratio, heat transfer coefficient, Nusselt number and enhanced heat transfer parameter as functions of oscillatory frequency and amplitude, Wormersely number and oscillating flow Reynolds number, respectively.

It is significant to note that heat transfer characteristics in oscillating flows in a channel with zero-mean can best be characterized by the oscillatory flow Reynolds number based on a half-cycle mean velocity, which is directly proportional to the product of the frequency and tidal displacement, and the channel

NOMENCLATURE

A, B, C	complex constants, equations (45)–(47), respectively
A_c	flow cross sectional area [m^2]
A_s	channel wall area [m^2]
a, b	channel wall thicknesses, see Fig. 1(b) [m]
C_1, C_2, C_3, C_4	complex constants
c_p	specific heat of fluid
f	frequency, $\omega/2\pi$ [Hz]
$f(y^*), g(y^*)$	complex functions of y^*
G	defined in equation (42)
H_j	defined in equation (27)
h	half height of flow channel [m]
h_m	average heat transfer coefficient [W m^{-2} K^{-1}]
i	$\sqrt{-1}$
J	defined in equation (26)
K	pressure gradient parameter [m s^{-2}]
k_1	thermal conductivity ratio of fluid to bottom wall
k_2	thermal conductivity ratio of fluid to top wall
k_f	thermal conductivity of fluid [W m^{-1} K^{-1}]
k_{s1}	thermal conductivity of bottom wall [W m^{-1} K^{-1}]
k_{s2}	thermal conductivity of top wall [W m^{-1} K^{-1}]
L	channel length [m]
M_j	defined in equation (24)
N_j	defined in equation (25)
Nu_m	average Nusselt number, $h_m 2h/k_f$
$Nu_{\Delta x}$	Nusselt number, $h_m \Delta x/k_f$
Pe	Peclet number, $Kh/\omega\alpha_f$
Pr	Prandtl number, ν/α_f
p	pressure [N m^{-2}]
Q	heat transfer rate [W]
Re_m	average Reynolds number, $u_m 2h/\nu$
$Re_{\Delta x}$	Reynolds number, $u_m \Delta x/\nu$
R_j	defined in equation (28)
S_j	defined in equation (29)
T	temperature [°C]
T'	periodic oscillatory component of temperature [°C]
t	time [s]
u	velocity in the x direction [m s^{-1}]
u_m	mean fluid velocity [m s^{-1}]
x, y	coordinates [m]
$\langle\ \rangle$	positive half-cycle time-average.

Greek symbols

α	Wormersley number
α_f	thermal diffusivity of fluid [m^2 s^{-1}]
α_{s1}	thermal diffusivity of bottom wall [m^2 s^{-1}]
α_{s2}	thermal diffusivity of top wall [m^2 s^{-1}]
β	heat flux parameter, $-\pi/2\gamma(\langle\partial T/\partial y\rangle)_{s1}$
γ	constant axial temperature gradient [°C m^{-1}]
Δx	tidal displacement [m]
Δx^*	nondimensional tidal displacement, $\Delta x\omega^2/2K$
ε_1	a/h
ε_2	b/h
θ	nondimension temperature difference ratio, equation (51)
ν	kinematic viscosity of fluid [m^2 s^{-1}]
ρ	density of fluid [kg m^{-3}]
σ_1	thermal diffusivity ratio of fluid to bottom wall
σ_2	thermal diffusivity ratio of fluid to top wall
Φ	defined in equation (49)
ω	oscillatory angular frequency [rad s^{-1}].

Superscripts

*	nondimensional variables, equation (13)
′	periodic fluctuation component of temperature
‾	complex conjugate.

Subscripts

f	fluid
j	1, 2
s1	bottom channel wall (heat flux side)
s2	top channel wall (insulated side).

height [9, 12]. Studies in refs. [9, 10, 12] deal with flows corresponding to moderate and intermediate Reynolds numbers, while those of Zhang and Kurzweg [2] and Kurzweg [5] are essentially for small or vanishing Reynolds numbers. It can be readily shown [12] that in the regime of vanishing Reynolds numbers, the flow is laminar and fully developed, and the problem is linear under the assumption of constant properties. The analysis presented in this paper belongs to this latter flow regime, and deals with an oscillating pressure gradient imposed across a parallel plate channel with the bottom wall heated and the top wall insulated. The heat capacity effects of both wall thicknesses are also accounted for.

MATHEMATICAL FORMULATION

A typical electronic chassis, as illustrated in Fig. 1(a), consists of a channeled enclosure containing several printed circuit boards (PCB) on which electronic components are mounted. Heat generated within an individual electronic component is transported to the

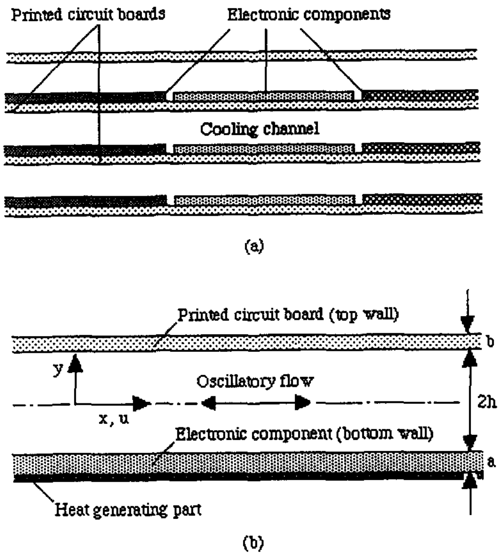

FIG. 1. Printed circuit boards in cooling channels (a) and simulation model (b).

solid walls surrounding it by conduction, and then to the cooling fluid medium by convection. The schematic of a simulation model for Fig. 1(a) is shown in Fig. 1(b). Uniform heat fluxes are provided at $y = -(h+a)$ and the dimension b represents half of the printed circuit board. Effects of unsteady heat conduction in both wall thicknesses a and b are also taken into account, and all thermal properties are taken to be constants. The fluid flow is laminar and two-dimensional, and the fluid is incompressible.

Under the additional conditions of fully developed flow and temperature fields and negligible viscous dissipation and pressure work, the governing equations take the following forms:

$$\frac{\partial u}{\partial t} = -\frac{1}{\rho}\frac{\partial p}{\partial x} + \nu\frac{\partial^2 u}{\partial y^2} \qquad -h \leqslant y \leqslant h \tag{1}$$

$$\frac{\partial T}{\partial t} + u\frac{\partial T}{\partial x} = \alpha_f\left(\frac{\partial^2 T}{\partial x^2} + \frac{\partial^2 T}{\partial y^2}\right) \qquad -h \leqslant y \leqslant h \tag{2}$$

$$\frac{\partial T}{\partial t} = \alpha_{s1}\left(\frac{\partial^2 T}{\partial x^2} + \frac{\partial^2 T}{\partial y^2}\right) \qquad -(h+a) \leqslant y \leqslant -h \tag{3}$$

$$\frac{\partial T}{\partial t} = \alpha_{s2}\left(\frac{\partial^2 T}{\partial x^2} + \frac{\partial^2 T}{\partial y^2}\right) \qquad h \leqslant y \leqslant (h+b) \tag{4}$$

where u is the longitudinal velocity, p is the static pressure, ρ is the fluid density, ν is the fluid kinematic viscosity, t is the time variable, x and y are the coordinates defined in Fig. 1(b), α_f and α_{s1} and α_{s2} are the thermal diffusivities of the fluid and walls, respectively.

The boundary conditions to the momentum equation (1) are $u = 0$ on the channel walls, and $\partial u/\partial x = 0$ along the channel centre line. The boundary conditions of the energy equations (2), (3) and (4) are as follows:

$$y = -(h+a): \quad \left(\left\langle\frac{\partial T}{\partial y}\right\rangle\right)_{s1} = \text{const.} \tag{5}$$

$$y = -h: \quad (T)_f = (T)_{s1}, \quad \left(k\frac{\partial T}{\partial y}\right)_f = \left(k\frac{\partial T}{\partial y}\right)_{s1} \tag{6}$$

$$y = h: \quad (T)_f = (T)_{s2}, \quad \left(k\frac{\partial T}{\partial y}\right)_f = \left(k\frac{\partial T}{\partial y}\right)_{s2} \tag{7}$$

$$y = (h+b): \quad \left(\frac{\partial T}{\partial y}\right)_{s2} = 0 \tag{8}$$

where $\langle\ \rangle$ refers to a positive half-cycle average quantity, the subscripts f and s denote quantities pertaining to the fluid and walls, respectively, also the subscripts 1 and 2 refer to the bottom wall and top wall, respectively. As we will only seek a long-time normal mode solution, the initial condition can be omited. It is also noted that the uniform heat flux condition at $y = -(h+a)$ is written in terms of a time-averaged normal temperature gradient. This is reasonable description since in a microelectronic component such as a chip, the heat flux is caused by heat generation in the substrate which occupies a small but nonzero volume.

ANALYTICAL SOLUTION

Here, we consider an oscillatory flow through a plane channel, in which the longitudinal pressure gradient caused, for example, by a motion of the piston is harmonic and given by

$$-\frac{1}{\rho}\frac{\partial p}{\partial x} = K\cos\omega t \tag{9}$$

where K is a constant pressure gradient parameter. Also, in a thermally developed region with uniform wall heat flux, all temperature rise will be linear in the downstream direction. Therefore, the temperature can be decomposed into two terms such that

$$T(x, y, t) = \gamma x + T'(y, t) \tag{10}$$

where the term T' is the periodic temperature fluctuation which behaves in a periodic oscillatory manner, and the term γx represents the non-periodic linear temperature rise where γ is a constant axial temperature gradient. From an energy balance, it may be shown that

$$\gamma = \frac{Q}{\rho u_m c_p A_c L} \tag{11}$$

where u_m is the half-cycle mean fluid velocity which can be evaluated by

$$u_m = \frac{1}{2h}\int_{-h}^{h}\langle u\rangle\,dy = \frac{1}{2h}\int_{-h}^{h}dy\,\frac{\omega}{\pi}\int_{\pi/\omega}^{2\pi/\omega}u(y,t)\,dt. \tag{12}$$

With the following nondimensional variables:

$$t^* = \omega t, \quad y^* = \frac{y}{h}, \quad u^* = \frac{u}{(K/\omega)} \tag{13}$$

and assuming that the velocity function and temperature function have the following forms, respectively:

$$u^* = f(y^*)\,e^{it^*} \tag{14}$$

$$T' = \gamma h g(y^*)\,e^{it^*} \tag{15}$$

where $i = \sqrt{(-1)}$, the solution to equation (1) with the velocity boundary conditions can be written as [13]

$$u^* = f(y^*)\,e^{it^*} = i\left[\frac{\cosh(\sqrt{(i)}\alpha y^*)}{\cosh(\sqrt{(i)}\alpha)} - 1\right]e^{it^*} \tag{16}$$

where $\alpha = h\sqrt{(\omega/\nu)}$ is a nondimensional parameter, commonly refered to as the Wormersley number, which represents the ratio of the channel height to the viscous diffusion length, or gives a measure of the ratio of inertial to viscous forces.

Substituting (10) into equations (2), (3) and (4), together with the boundary conditions (5)–(8), we obtain the analytical solution of these equations as follows:

$$g_f(y^*) = \frac{iPe}{\alpha^2(Pr-1)}f(y^*) - \frac{Pe}{\alpha^2 Pr\,(Pr-1)} + C_1\cosh(\sqrt{(iPr)}\alpha y^*) + iC_2\sinh(\sqrt{(iPr)}\alpha y^*) \tag{17}$$

$$g_{s1}(y^*) = C_3\cosh[\sqrt{(i\sigma_1 Pr)}\alpha(y^*+1+\varepsilon_1)] - \frac{\beta\sinh[\sqrt{(i\sigma_1 Pr)}\alpha(y^*+1)]}{\sqrt{(i\sigma_1 Pr)}\alpha\cosh[\sqrt{(i\sigma_1 Pr)}\alpha\varepsilon_1]} \tag{18}$$

and

$$g_{s2}(y^*) = C_4\cosh[\sqrt{(i\sigma_2 Pr)}\alpha(y^*-1-\varepsilon_2)] \tag{19}$$

where g_f, g_{s1} and g_{s2} represent the y^*-dependent temperature functions within the fluid and within the electronic component and PCB wall, respectively, $\sigma_1 = \alpha_f/\alpha_{s1}$ is the thermal diffusivity ratio of fluid to bottom wall (see Fig. 1(b)), $\sigma_2 = \alpha_f/\alpha_{s2}$ is the thermal diffusivity ratio of fluid to top wall, $Pr = \nu/\alpha_f$ is the fluid Prandtl number, $Pe = Kh/\omega\alpha_f$ is the Peclet number, $\varepsilon_1 = a/h$ and $\varepsilon_2 = b/h$, β is the imposed heat flux parameter defined as $\beta = -(\pi/2\gamma)(\langle\partial T/\partial y\rangle)_{s1}$. The constants C_1, C_2, C_3 and C_4 are determined by the conditions (5)–(8). They are

$$C_4 = \left[-\frac{Pe}{\alpha^2 Pr(Pr-1)} + C_1\cosh(\sqrt{(iPr)}\alpha) + iC_2\sinh(\sqrt{(iPr)}\alpha)\right]\frac{1}{\cosh(\sqrt{(i\sigma_2 Pr)}\alpha\varepsilon_2)} \tag{20}$$

$$C_3 = \left[-\frac{Pe}{\alpha^2 Pr(Pr-1)} + C_1\cosh(\sqrt{(iPr)}\alpha) - iC_2\sinh(\sqrt{(iPr)}\alpha)\right]\frac{1}{\cosh(\sqrt{(i\sigma_1 Pr)}\alpha\varepsilon_1)} \tag{21}$$

and

$$iC_2 = \frac{(N_2-N_1-J)}{(M_1+M_2)} \tag{22}$$

$$C_1 = N_1 + J + (N_2-N_1-J)\frac{M_1}{(M_1+M_2)} \tag{23}$$

where

$$M_j = \frac{H_j}{R_j} \quad j = 1,2 \tag{24}$$

$$N_j = \frac{Pe}{\alpha^2 Pr(Pr-1)\cosh(\sqrt{(iPr)}\alpha)}\frac{S_j}{R_j} \quad j = 1,2 \tag{25}$$

$$J = -\frac{\beta\sinh(\sqrt{(i\sigma_1 Pr)}\alpha\varepsilon_1)[\tanh(\sqrt{(i\sigma_1 Pr)}\alpha\varepsilon_1) - \operatorname{ctnh}(\sqrt{(i\sigma_1 Pr)}\alpha\varepsilon_1)]}{\sqrt{(iPr)}\alpha\cosh(\sqrt{(iPr)}\alpha)R_1} \tag{26}$$

and

$$H_j = k_j + \sqrt{\sigma_j}\tanh(\sqrt{(iPr)}\alpha) \times\tanh(\sqrt{(i\sigma_j Pr)}\alpha\varepsilon_j) \quad j = 1,2 \tag{27}$$

$$R_j = k_j\tanh(\sqrt{(iPr)}\alpha) + \sqrt{(\sigma_j)}\tanh(\sqrt{(i\sigma_j Pr)}\alpha\varepsilon_j) \quad j = 1,2 \tag{28}$$

$$S_j = k_j\sqrt{(Pr)}\tanh(\sqrt{(i)}\alpha) + \sqrt{(\sigma_j)}\tanh(\sqrt{(i\sigma_j Pr)}\alpha\varepsilon_j) \quad j = 1,2 \tag{29}$$

where $k_1 = k_f/k_{s1}$ is the thermal conductivity ratio of fluid to bottom wall, $k_2 = k_f/k_{s2}$ is the thermal conductivity ratio of fluid to top wall.

If there is no heat flux at the bottom wall, then $\beta = 0$ and $J = 0$, and if $k_1 = k_2 = k$, $\sigma_1 = \sigma_2 = \sigma$ and $\varepsilon_1 = \varepsilon_2 = \varepsilon$, then $M_1 = M_2 = M$, $N_1 = N_2 = N$, then the solutions given above can be simplified, resulting in

$$C_1 = N = \frac{Pe}{\alpha^2 Pr(Pr-1)\cosh(\sqrt{(iPr)}\alpha)} \times\frac{k\sqrt{(Pr)}\tanh(\sqrt{(i)}\alpha) + \sqrt{(\sigma)}\tanh(\sqrt{(i\sigma Pr)}\alpha\varepsilon)}{k\tanh(\sqrt{(iPr)}\alpha) + \sqrt{(\sigma)}\tanh(\sqrt{(i\sigma Pr)}\alpha\varepsilon)} \tag{30}$$

$$C_2 = 0 \tag{31}$$

and

$$C_3 = C_4 = \left[-\frac{Pe}{\alpha^2 Pr(Pr-1)} + C_1\cosh(\sqrt{(iPr)}\alpha)\right]\frac{1}{\cosh(\sqrt{(i\sigma Pr)}\alpha\varepsilon)} \tag{32}$$

and

$$g_f(y^*) = \frac{iPe}{\alpha^2(Pr-1)} f(y^*) - \frac{Pe}{\alpha^2 Pr(Pr-1)} + C_1 \cosh(\sqrt{(iPr)}\alpha y^*) \quad (33)$$

$$g_{s1}(y^*) = C_3 \cosh[\sqrt{(iPr)}\alpha(y^*+1+\varepsilon)] \quad (34)$$

$$g_{s2}(y^*) = C_4 \cosh[\sqrt{(iPr)}\alpha(y^*-1-\varepsilon)]. \quad (35)$$

The expressions (30)–(35) are identical to the results given by Kurzweg [5]. To facilitate the discussion of the physical phenomena given by the analytical solution, several pertinent quantities can also be derived, and are given in the following.

Mean Reynolds number and tidal displacement

As already mentioned previously, the oscillatory flow Reynolds number Re_m is one of the two essential dimensionless parameters characterizing the flow studied here. It is defined on the basis of the half-cycle mean velocity u_m given in equation (12) and the channel height, $2h$. The characteristic velocity u_m is directly proportional to the frequency of the oscillatory flow and its tidal displacement Δx, which is commonly taken to be the cross-stream maximum excursion of fluid particles during one oscillation cycle. A second parameter is either the Wormersley number α or the tidal displacement parameter given by $\Delta x/h$. Their relationship can be seen by the following:

$$\Delta x = \frac{1}{2h}\int_{\pi/\omega}^{2\pi/\omega} dt \int_{-h}^{h} u(y,t)\, dy = \frac{2K}{\omega^2}\left[1 - \frac{\sqrt{(2)}\sin\left(\frac{\alpha}{\sqrt{2}}\right)\cos\left(\frac{\alpha}{\sqrt{2}}\right)}{\alpha\left[\cosh^2\left(\frac{\alpha}{\sqrt{2}}\right)\cos^2\left(\frac{\alpha}{\sqrt{2}}\right) + \sinh^2\left(\frac{\alpha}{\sqrt{2}}\right)\sin^2\left(\frac{\alpha}{\sqrt{2}}\right)\right]}\right]. \quad (36)$$

In addition, it is desirable to note the following identities:

$$u_m = 2f\Delta x \quad (37)$$

$$Re_m = \frac{u_m 2h}{\nu} = \frac{4f\Delta x h}{\nu} = \frac{2\alpha^2}{\pi}\frac{\Delta x}{h} \quad (38)$$

$$\beta = \frac{\pi}{2} k_1 Re_m Pr \quad (39)$$

where f is $\omega/2\pi$.

Mean heat transfer coefficient and Nusselt number

The parameters of interest in cooling of electronic equipment are the heat transfer coefficient on the component surface, and the temperature variation in the fluid and in the heat generating area. The average heat transfer coefficient on the component surface, h_m, is defined as

$$h_m = \frac{Q}{A_s(\langle T'_{s1}\rangle - T'_b)} \quad (40)$$

where $\langle T'_{s1}\rangle$ is the time-average surface temperature excess of the bottom wall, and T'_b is the average bulk temperature excess of the fluid. In terms of the analytical solution given in equations (17) and (18), the $\langle T'_{s1}\rangle$ can be calculated by

$$\langle T'_{s1}\rangle = \frac{\gamma h}{\pi}[G+\bar{G}+i(G-\bar{G})] \quad (41)$$

where

$$G = -\frac{Pe}{\alpha^2 Pr(Pr-1)} + C_1\cosh(\sqrt{(iPr)}\alpha) - iC_2\sinh(\sqrt{(iPr)}\alpha). \quad (42)$$

Here the bars designate the complex conjugate. The bulk temperature excess T'_b is defined as

$$T'_b = \frac{\int_{-1}^{1}\langle uT'\rangle\, dy^*}{\int_{-1}^{1}\langle u\rangle\, dy^*}. \quad (43)$$

Substituting the explicit forms for $f(y^*)$ and $g_f(y^*)$ into (43) and then performing the integration yields

$$T'_b = \frac{\pi\gamma h}{16\Delta x^*\alpha^2(Pr+1)}\left[A\bar{C}+\bar{A}C+\frac{1}{Pr}(B+\bar{B})\right] \quad (44)$$

where

$$A = \sqrt{(i)}\alpha\tanh(\sqrt{(i)}\alpha) \quad (45)$$

$$B = -\frac{2PeA}{\alpha^2(Pr-1)} + 2C_1\sqrt{(iPr)}\alpha\sinh(\sqrt{(iPr)}\alpha) \quad (46)$$

$$C = -\frac{2Pe}{\alpha^2(Pr-1)} + 2C_1\cosh(\sqrt{(iPr)}\alpha). \quad (47)$$

Using the formulas (41) and (44), together with the definition of the axial temperature gradient γ given by (11), yields the following expression for the average heat transfer coefficient:

$$h_m = \frac{k_f Re_m Pr}{h\Phi} \quad (48)$$

where

$$\Phi = \frac{1}{\pi}[G+\bar{G}+i(G-\bar{G})] - \frac{\pi}{16\Delta x^*\alpha^2(Pr+1)}\left[A\bar{C}+\bar{A}C+\frac{1}{Pr}(B+\bar{B})\right]. \quad (49)$$

The Nusselt number expression based on $2h$ is then

$$Nu_m = \frac{h_m 2h}{k_f} = \frac{2}{\Phi}Re_m Pr. \quad (50)$$

It is noted that the nondimensional tidal displacement $\Delta x^* = \Delta x/(2K/\omega^2)$ depends only on α in accordance with (36), and the Φ in the above equation is a function of α, Re_m, and Pr.

RESULTS AND DISCUSSION

Before results are calculated, it is necessary to specify property ratios and geometrical parameters that are pertinent to the electronic cooling problem considered here. These include the thermal conductivity ratios, k_1 and k_2, the thermal diffusivity ratios, σ_1 and σ_2, the Prandtl number, Pr, and the geometrical parameters, ε_1 and ε_2. Air is commonly used as a cooling medium. To reduce the external thermal resistance further, however, increasing emphasis is being placed on the use of liquid cooling technologies. When the heat dissipation from the electronic equipment is higher than 1000 W m^{-2}, immersion forced convection cooling by liquid, such as water and freon, is used [1]. Epoxy resins and silicone material are often used as sealant and insulation for electronic equipment. In this paper, we have obtained the solutions for different Wormersely numbers, ranging from about 0.1 to 2.0 for fluids with $Pr = 0.7$, corresponding to air and $Pr = 6.0$, corresponding to water. We have also made calculations for the following two cases with parameters pertinent to the physical problem [14]: $k_1 = 0.002$, $k_2 = 0.0016$, $\sigma_1 = 2.6$, $\sigma_2 = 2.3$, $\varepsilon_1 = 0.3$, $\varepsilon_2 = 0.2$ for air as coolant, and $k_1 = 0.05$, $k_2 = 0.04$, $\sigma_1 = 0.0172$, $\sigma_2 = 0.15$, $\varepsilon_1 = 0.3$, $\varepsilon_2 = 0.2$ for water as coolant. It is understood that these choices are somewhat arbitrary, but do provide a reasonable basis for discussing the physical phenomena.

Figure 2 illustrates the dependence of the average Nusselt number Nu_m given in equation (50) on the Wormersley number α. It is interesting to note that the average Nusselt number is specifically independent of the oscillatory flow Reynolds number. This is, however, somewhat expected, since a fully-developed thermal field is considered here. In addition, the solution presented here is for the case of vanishing oscillating

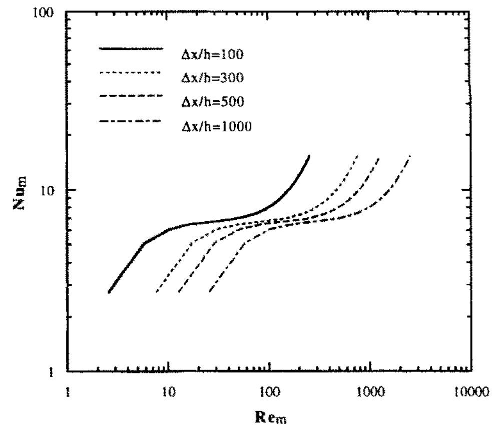

FIG. 3. Variations of average Nusselt number of air as a function of the oscillatory flow Reynolds number for different $\Delta x/h$.

Reynolds number, and therefore their effects should no longer be an issue. It is also interesting to note in Fig. 2 that at low α-values, the behaviors of Nu_m for air and water are quite different, while they deviate little from each other for the high α-values. A plausible reason for the different behaviors in the lower α region, which is related to the conduction effects in the bottom wall, will be described later in conjunction with the result on temperature profiles.

When the Wormersely number is expressed in terms of the tidal displacement parameter $\Delta x/h$, it is still possible to show the relation between Nu_m and Re_m as given in Fig. 3 for air and in Fig. 4 for water. These results are from the same data as those given in Fig. 2, but show more clearly the individual effects of Re_m and $\Delta x/h$ on the average Nusselt number Nu_m. These same results can be plotted in another way to show the extent of heat transfer enhancement possible by utilizing oscillatory flows. This is shown in Fig. 5 for both air and water. It is seen that as $\alpha > 0.4$ for air and as $\alpha > 0.9$ for water, heat transfer enhancement

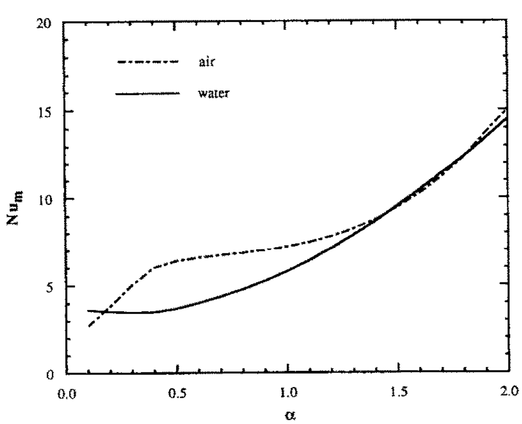

FIG. 2. Variations of average Nusselt number as function of Wormersley number for air and water.

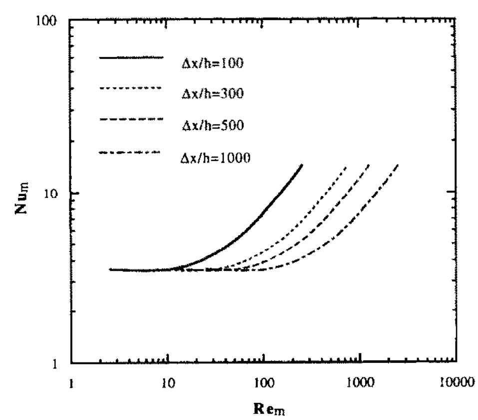

FIG. 4. Variations of average Nusselt number of water as a function of the oscillatory flow Reynolds number for different $\Delta x/h$.

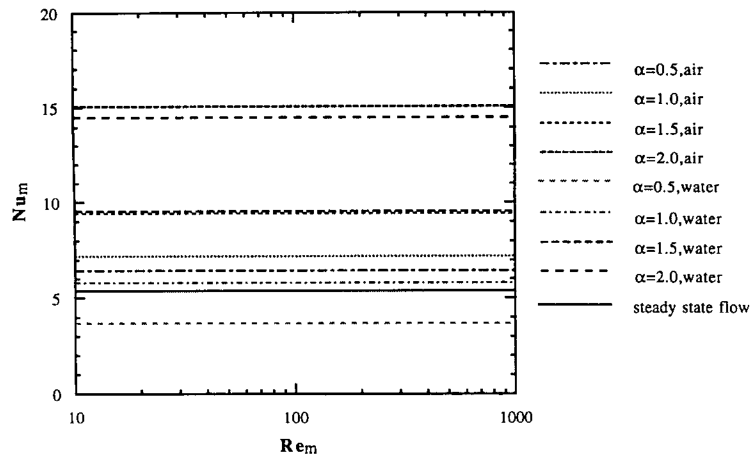

FIG. 5. Comparison of average Nusselt numbers to that of steady-flow.

is possible, since the Nu_m would then exceed a value of 5.38 for the case of steady laminar flow in a channel with uniform heat flux on one wall [15]. For $\alpha = 2.0$, the average Nusselt number is seen to be about 3 times that of the steady flow case.

Another interesting result on the heat transfer behavior can be obtained by introducing a different set of Reynolds and Nusselt numbers, $Re_{\Delta x} = u_m \Delta x/\nu$ and $Nu_{\Delta x} = h_m \Delta x/k_f$, with the tidal displacement Δx as the characteristic lengths. A plot of $Nu_{\Delta x}$ against $Re_{\Delta x}$ with α as the parameter is shown in Fig. 6 and a power relation between the two parameters at any given α clearly exists. In addition, the power is almost the same for all α, even though the constants in the power relations do not vary monotonically with α.

It is now appropriate to examine the time-dependent temperature profiles within each oscillation cycle. In the thermally fully-developed region under uniform heat flux at one wall, it is convenient to introduce a dimensionless temperature difference ratio as follows:

$$\theta = \frac{\langle T'_{s1} \rangle - T'}{\langle T'_{s1} \rangle - T'_b} \tag{51}$$

which is expected to be independent of the x-coordinate, similar to the corresponding case of steady laminar flow. For the y^*-region occupied by the fluid medium, the θ-profiles at various t^* values within an oscillation cycle are shown in Fig. 7 for air and in Fig. 8 for water, both for an α-value of 2.0.

In the case of air as a cooling medium, Fig. 7 shows that θ becomes essentially zero at the two boundaries of the fluid medium, indicating the fact that the temperature variations in the two wall thicknesses are

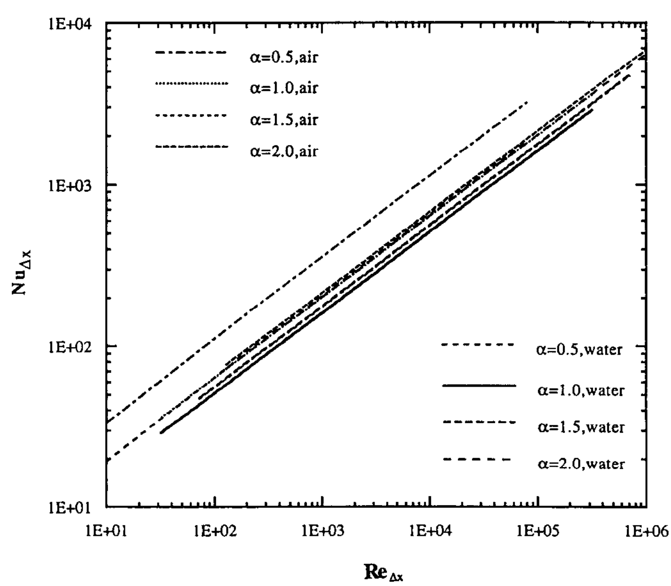

FIG. 6. $Nu_{\Delta x} - Re_{\Delta x}$ correlations for air and water.

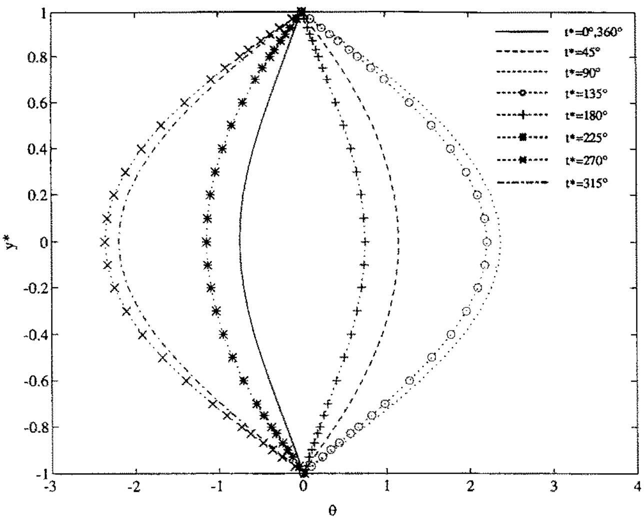

FIG. 7. Time-dependent temperature profiles within a cycle for air at $\alpha = 2.0$.

negligibly small and thus do not play an important role in affecting the temperature field in the fluid. The reason here is that the thermal conductivity of the wall material is so much larger than that of the air. Also it may be noted in Fig. 7 that despite the appearance of symmetrical oscillations of the θ-profile, these profiles are not strictly symmetrical with respect to the channel center line at $y^* = 0$, because of the imposed wall heat flux condition at $y = -(h+a)$. Figure 8 shows the corresponding θ-profiles for water, which are seen to be very different from those in Fig. 7. Here the thermal conductivity of water is only slightly lower than that of the wall materials, and thus conduction in the bottom wall plays an extremely important role in affecting the heat transfer and the temperature profiles. Interestingly, the time-dependent profiles are nearly symmetric about the line at $\theta = 1.0$. What this implies is that at the top wall, which is insulated at $y = h+b$, the wall surface temperature excess T'_{s2} is essentially the same as the bulk temperature excess of the fluid T'_b, thus indicating a very slight heat transfer at $y = h$. It is also interesting to note that in the regions around $y^* = -0.5$, temperature oscillations nearly die out and the temperature there remains essentially at the bulk temperature level, giving the appearance of the existence of standing waves. Figure 8 also shows the bottom wall surface temperature amplitudes at $y^* = -1.0$, which in the practical situation would correspond to the electronic component temperatures which need to be determined from a thermal management point of view. The relative conduction effects for air and water just discussed are the likely reason for the fact that the Nusselt numbers for air are higher than those for water in the lower α region as shown in Fig. 2. The added thermal resistance in the bottom wall thickness

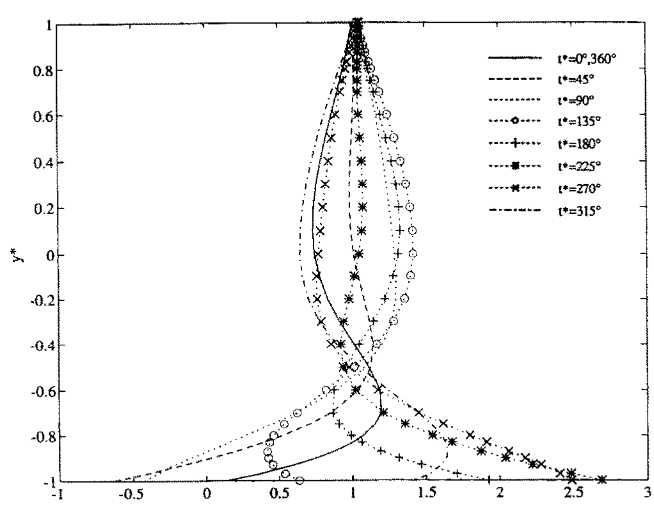

FIG. 8. Time-dependent temperature profiles within a cycle for water at $\alpha = 2.0$.

in the case of water reduces the wall surface temperature, thus also reducing the Nusselt number. Based on the above discussion, it can be concluded that in general if liquid cooling is used, wall conduction effects become very important in the prediction of junction temperatures in the case that the electronic component is a microelectronic chip.

CONCLUDING REMARKS

An exact solution is presented in this paper for the laminar fully-developed zero-mean oscillatory flow in a channel and heat transfer from one wall uniformly heated to simulate the forced convection cooling of electronic component on circuit boards in an open enclosure. This solution is valid for small oscillatory flow Reynolds number and the interaction with wall regions is also accounted for. Results are given in terms of time-averaged Nusselt number and time-dependent temperature profiles within an oscillatory cycle. Numerical data are provided for two specific cases of using air and water as the cooling media, based on properties and geometrical factors pertinent to the electronic enclosure problem, and for a range of Wormersely number from about 0.1 to 2.0. Based on these results, several conclusions can be drawn as follows.

1. The time-averaged Nusselt number for a given fluid is only a function of the Wormersely number α, and is specifically independent of the oscillatory flow Reynolds number. In the region of low α-values, the average Nusselt number for air is higher than that for water, and this difference is essentially due to the conduction effect inside the bottom wall thickness.

2. Heat transfer enhancement in the oscillatory flow case over the steady-flow case is found to be realizable when α is greater than 0.4 for air and 0.9 for water. A maximum of enhancement of the order of 200% over the steady-flow case has been found at $\alpha = 2.0$.

3. When the tidal displacement Δx is used as the characteristic length in both the average Nusselt number and the oscillatory flow Reynolds number, $Nu_{\Delta x}$ becomes a power function of $Re_{\Delta x}$ with essentially the same power for all values of α and both fluid media.

4. For air, the temperature variations in the wall thicknesses are very slight, while those for water are significantly larger. If the results were to predict chip junction temperatures, neglecting the conduction effect in the wall could lead to substantial error in the case of using liquid as a coolant.

This study is a part of a larger study dealing with enhanced cooling of electronic components and enclosures by means of zero-mean oscillatory flows over the complete regime of oscillatory flow Reynolds numbers. This study specifically addresses the low and vanishing oscillatory flow Reynold number. Preliminary results for intermediate and high oscillatory flow Reynolds number are given in refs. [9, 10, 12], and additional studies in these regions are currently continuing and results will be reported in due time.

Acknowledgement—The authors are grateful to the IBM corporation, Endicott, NY, for funding the study.

REFERENCES

1. F. P. Incropera, Convection heat transfer in electronic equipment cooling, *J. Heat Transfer* **110,** 1097–1111 (1980).
2. J. G. Zhang and U. H. Kurzweg, Numerical Simulation of time-dependent heat transfer in oscillatory pipe flow, *J. Thermophys.* **5,** 401–406 (1991).
3. M. Kaviany, Performance of a heat exchanger based on enhanced heat diffusion in fluids by oscillation: analysis, *J. Heat Transfer* **112,** 49–55 (1990).
4. M. Kaviany and M. Reckker, Performance of a heat exchanger based on enhanced heat dfiffusion in fluids by oscillation: experiment, *J. Heat Transfer* **112,** 56–63 (1990).
5. U. H. Kurzweg, Enhanced heat conduction in oscillating viscous flows within parallel-plate channels, *J. Fluid Mech.* **156,** 291–300 (1985).
6. G. E. Karniadakis, B. B. Mikic and A. T. Patera, Heat transfer enhancement by flow destabilization: application to the cooling of chips, *Cooling Technology for Electronic Equipment* (Edited by W. Aung) p. 587. Hemisphere, New York (1988).
7. C. H. Amon, Numerical prediction of convective heat transfer in self-sustained oscillatory flow, *J. Thermophys.* **4,** 239–246 (1990).
8. C. H. Amon, Heat transfer enhancement by flow destabilization in electronic chip configurations, *J. Electronic Packaging* **114,** 35–40 (1992).
9. W. L. Cooper, V. W. Nee and K. T. Yang, An experimental investigation of convective heat transfer from the heated floor of a rectangular duct to a low frequency, large tidal displacement oscillatory flow, *Int. J. Heat Mass Transfer* **37,** 581–592 (1994).
10. T. E. Walsh, K. T. Yang, V. W. Nee and Q. D. Liao, Forced convection cooling in microelectronic cabinets via oscillatory flow techniques, *Proceeding of the 3rd World Conference on Experimental Heat Transfer, Fluid Mechanics and Thermodynamics*, pp. 641–648, Nov. (1993).
11. Q. D. Liao, V. W. Nee and K. T. Yang, Experimental study of enhanced heat transfer in microcomputer cabinets with channelled oscillatory air flow, *1st International Conference on Flow Interaction*, Hong Kong (1994) (to appear).
12. H. J. Huang, Heat transfer enhancement in an open enclosure by zero-mean oscillatory flows at small and intermediate oscillatory flow Reynolds numbers, Ph.D. Dissertation, University of Notre Dame (1994).
13. R. L. Panton, *Incompressible Flow*. Wiley, New York (1984).
14. C. A. Harper, *Handbook of Materials and Processes for Electronics*. McGraw-Hill, New York (1978).
15. R. K. Shah and A. L. London, *Laminar Flow Forced Convection in Ducts*. Academic Press, New York (1978).